3   ELECTRIC AND MAGNETIC FIELDS INSIDE THE BODY

3.1   Introduction

Chapter 2 describes the fields to which people are exposed. Exposure to these fields in turn induces fields and currents inside the body. This chapter describes and quantifies the relationship between external fields and contact currents with the current density and electric fields induced within the body. Only the induced electric field and resultant current density in tissues and cells are considered, as the internal magnetic field in tissues and cells is the same as the external field. The chapter first considers calculations on a macroscopic scale referring to dimensions much greater than those of cells or cell assemblies, and then on a microscopic scale when dimensions considered are comparable to, or smaller than a cell.

At extremely low frequencies, exposure is characterized by the electric field strength (E) or the electric flux density (also called the displacement) vector (D), and the magnetic field strength (H) or the magnetic flux density (also called the magnetic induction) (B). All these parameters are vectors; vectors are denoted in italics in this Monograph (see also paragraph 2.1.1). The flux densities are related to the field strengths by the properties of the medium in a given location r as:

$$D(r) = \hat{\varepsilon}\, E(r)$$
$$B(r) = \hat{\mu}\, H(r)$$

where $\hat{\varepsilon}$ is the complex permittivity and $\hat{\mu}$ is the permeability. For biological media $\hat{\mu} \cong \mu_0$ where μ_0 is the permeability of free space (air). The electric and magnetic fields are effectively decoupled, since quasi-static conditions can be assumed (Olsen, 1994). To determine exposure in a given location, both the electric and magnetic field have to be computed or measured separately. Similarly, the internal induced fields are also evaluated separately. For simultaneous exposure to electric and magnetic fields, the internal measures can be obtained by superposition. Exposures to either electric or magnetic fields result in the induction of electric fields and associated current density in conductive tissue. The magnitudes and spatial patterns of these fields depend on the type of the exposure field (electric vs. magnetic), their characteristics (frequency, magnitude, orientation, etc.), and the size, shape, and electrical properties of the exposed body (human, animal). A biological body significantly perturbs an external electric field, and the exposure also results in an electric charge on the body surface. The external electric field is also strongly perturbed by metallic or other conductive objects.

The primary dosimetric measure is the local induced electric field. This measure is selected because thresholds of the excitable tissue stimulation are defined by the electric field and its spatial variation. However, current density is used in some exposure guidelines (ICNIRP, 1998a). Among the measurements often reported are the average, root mean square (rms) and maximum induced electric field and current density values (Stuchly & Daw-

son, 2000). Additional measurements more recently introduced are the 50th, 95th, and 99th percentiles, which indicate values not exceeded in the given volume of tissue, e.g. the 99th percentile shows the dosimetric measure exceeded in 1% of a given tissue volume (Kavet et al., 2001). Some exposure guidelines (ICNIRP, 1998a) specify dosimetry limit values as current density averaged over 1 cm^2 of tissue. The electric field in tissue is typically expressed in V m^{-1} or mV m^{-1} and the current density in A m^{-2} or mA m^{-2}.

The internal (induced) electric field (E) and conduction current density (J) are related through Ohm's law:

$$J = \sigma E$$

where σ is the bulk tissue conductivity, and may be a tensor in anisotropic tissues (e.g. muscle).

Early dosimetry modeled a human body as homogeneous ellipsoids or other overly simplified shapes. In addition, limited measurements of currents through the whole body and body parts have been performed. During the last few years, a few research laboratories have performed extensive computations of the induced electric field and current density in heterogeneous models of the human body in uniform and non-uniform electric or magnetic fields at 50 or 60 Hz. There is convergence of the results obtained by various groups and agreement with earlier measurements, where such measurements are available (Caputa et al., 2002; Stuchly & Gandhi, 2000). Microscopic dosimetry data remain very limited.

3.2 Models of human and animal bodies

Currently, a number of laboratories have developed heterogeneous models of the human body with realistic anatomy and numerous tissues identified. Most of these models have been developed by computer segmentation of data from magnetic resonance imaging (MRI) and allocation of proper tissue type (Dawson, 1997; Dawson, Moerloose & Stuchly, 1996; Dimbylow, 1997; Dimbylow, 2005; Gandhi, 1995; Gandhi & Chen, 1992; Zubal, 1994). Special care has been taken to make these models anatomically realistic. Table 22 summarizes essential characteristics of some of these models.

Typically, over 30 distinct organs and tissues are identified and represented by cubic cells (voxels) of 1 to 10 mm on a side. Voxels are assigned a conductivity value based on measured values for various organs and tissues (Gabriel, Gabriel & Corthout, 1996). A human body model constructed from several geometrical bodies of revolution has also been used (Baraton, Cahouet & Hutzler, 1993; Hutzler et al., 1994). The model is symmetric and is divided into about 100000 tetrahedral elements, which represent only the major organs. This can be contrasted with over eight million of tissue voxels used in the hybrid method with resolution of 3.6 mm (Dawson, Caputa & Stuchly, 1998). In the hybrid method, the FDTD part of the modeling requires that the body model is enclosed in a parallelepiped. To illustrate the

quality of such models Figure 1 shows the external view, the skeleton and skin, and the main internal organs.

Table 22. Main characteristics of the MRI-derived models of the human body

Model	NRPB [a]	University of Utah [b]	University of Victoria [c]
Height and mass	1.76 m, 73 kg	1.76 m, 64 kg scaled to 71 kg	1.77 m, 76 kg
Original voxels	2.077 x 2.077 x 2.021 mm	2 x 2 x 3 mm	3.6 x 3.6 x 3.6 mm
Posture	upright, hands at sides	upright, hands at sides	upright, hands in front

[a] Source: Dimbylow, 1997.

[b] Source: Gandhi & Chen, 1992.
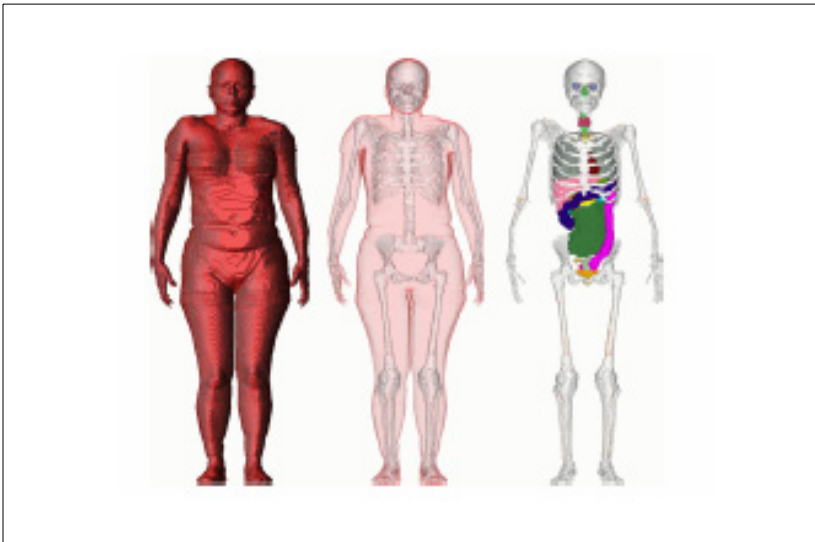
[c] Source: Dawson, 1997.

Figure 1. Volume rendered images of a female voxel phantom (NAOMI). In the image on the left the opacity of the skin has been hardened and the image is illuminated to display the outside surface. In the middle image the opacity of the skin has been reduced to enable the internal skeleton to be seen. The image on the right shows the skeleton and internal organs. The skin, fat, muscle and breasts have been removed. (Dimbylow, 2005)

A few animal models, namely rats, mice and monkeys have also been developed. The quality of the models varies.

3.3   Electric field dosimetry

3.3.1   Basic interaction mechanisms

As mentioned earlier the human (or animal) body significantly perturbs a low-frequency electric field. In most practical cases of human exposure, the field is vertical (with respect to the ground). At low frequencies, the body is a good conductor, and the electric field is nearly normal to its surface. The electric field inside the body is many orders of magnitude smaller than the external field. Non-uniform charges are induced on the surface of the body and the current direction inside the body is mostly vertical. Figure 2 illustrates the electric fields in air around the human body and body surface charge density for the model in free space and on perfect ground.
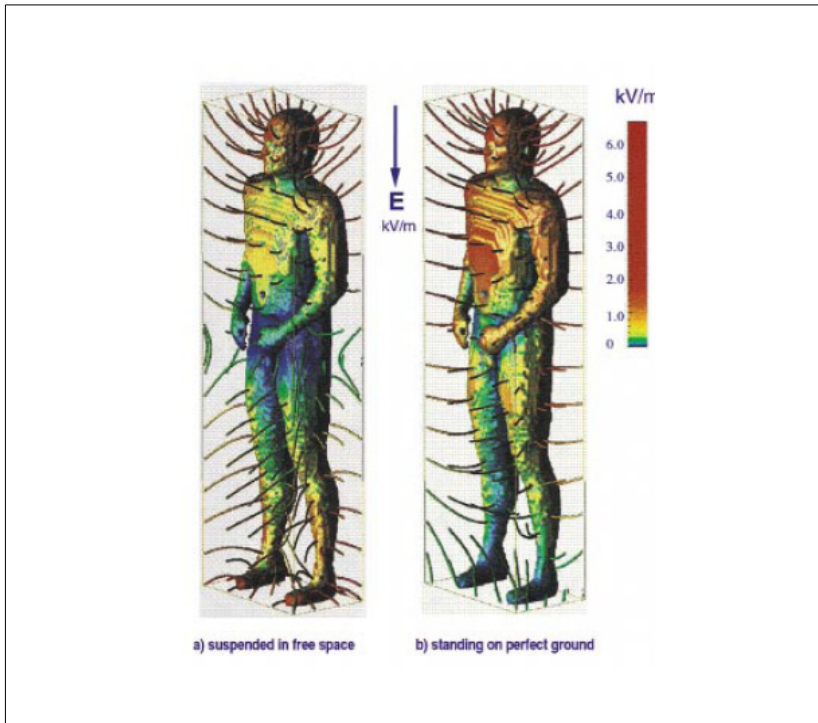

Figure 2. Human body in a uniform electric field of 1 kV m^{-1} at 60 Hz showing the external electric field and surface charge density on the body surface: (a) in free space, and (b) in contact with perfect ground (Stuchly & Dawson, 2000).

The electric field in the body strongly depends also on the contact between the body and the electric ground, where the highest fields are found when the body is in perfect contact with ground through both feet (Deno & Zaffanella, 1982). The further away from the ground the body is located, the

lower the electric fields in tissues. For the same field, the maximum ratio of internal fields for grounded to free space models is about two.

3.3.2 Measurements

Kaune & Forsythe (1985) performed measurements of currents in models consisting of manikins standing in a vertical electric field with both feet grounded. The model was filled with saline solution whose conductivity is equal to that of the average human tissues. The results of the measurements are shown in Figure 3.
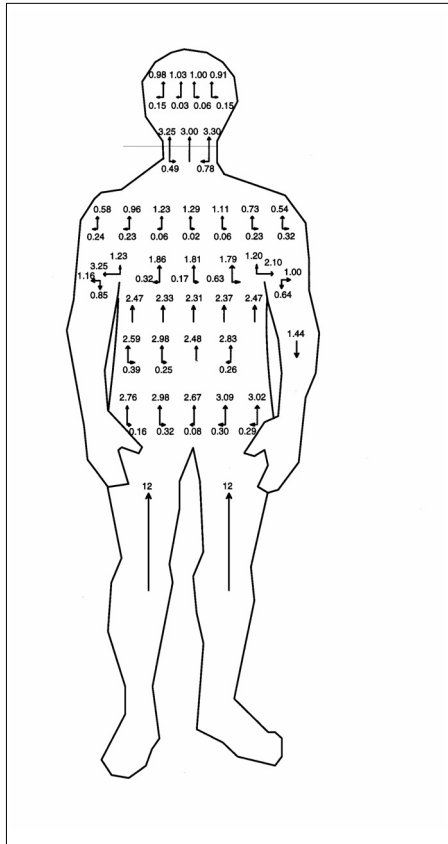

Figure 3. Measured current density (mA m^{-2}) in a saline filled homogeneous phantom grounded through both feet. The electric field strength is 10 kV m^{-1}, the field vector is directed along the long axis of the body, and the frequency is 60 Hz (Kaune & Forsythe, 1985).

3.3.3 Computations

Early dosimetry computations represented the human (or animal) body as a homogeneous body of revolution with a single conductivity value.

Examples of analytic solutions in homogeneous geometric shapes for electric field exposure are available in Shiau & Valentino (1981), Kaune and McCreary (1985), Tenforde & Kaune (1987), Spiegel (1977), Foster and Schwan (1989) and Hart (1992). Measurements of currents within the body have also been performed (Deno & Zaffanella, 1982; Kaune & Forsythe, 1985; Kaune, Kistler & Miller, 1987). As an intermediate development, highly simplified body-like shapes have been evaluated by numerical methods (Chen, Chuang & Lin, 1986; Chiba et al., 1984; Dimbylow, 1987; Spiegel, 1981).

Various computational methods have been used to evaluate induced electric fields in high-resolution models. Computations of exposure to electric fields are generally more difficult than for the magnetic field exposure, since the human body significantly perturbs the exposure field. Suitable numerical methods are limited by the highly heterogeneous electrical properties of the human body and equally complex external and organ shapes. The methods that have been successfully used so far for high-resolution dosimetry are the finite difference (FD) method in frequency domain and time domain (FDTD) and the finite element method (FEM). Each method and its implementation offer some advantages and have limitations, as reviewed by Stuchly and Dawson (2000). Some of the methods and computer codes have undergone extensive verification by comparison with analytic solutions (Dawson & Stuchly, 1996; Stuchly et al., 1998). An extensive valuation of accuracy of various dosimetric measures is also available (Dawson, Potter & Stuchly, 2001).

Several numerical computations of the electric field and current density induced in various organs and tissues have been performed (Dawson, Caputa & Stuchly, 1998; Dimbylow, 2000; Furse & Gandhi, 1998; Hirata et al., 2001). In a more recent publication (Dimbylow, 2000), the maximum current density is averaged over 1 cm^2 for excitable tissues. The latter computation is clearly aimed at compliance with the most recent ICNIRP guideline (ICNIRP, 1998a and a later published clarification on tissue-related applicability of the limit (ICNRIP, 1998b).

Effects of two sets of conductivity have been examined in high-resolution models (Dawson, Caputa & Stuchly, 1998). The difference between calculation with either set is negligible on short-circuit current and very small on the average and maximum electric field and current density values in horizontal slices of the body. This conclusion is in agreement with the basic physical laws as explained by Dawson, Caputa & Stuchly (1998). The average and maximum electric fields vary, but less than the induced current density values for the same organ for the two different sets of conductivity. It is also apparent that not only the conductivity of a given organ determines its current density, but also the conductivity of other tissues. In general, lower induced electric fields (higher current density) are associated with higher conductivity of tissue. The exceptions are locations in the body associated with the concave curvature, e.g. tissue surrounding the armpits, where the electric field is enhanced. For the whole-body the averages are within 2%.

The maximum values of the electric field differ by up to 20% for the two sets of conductivity.

Model resolution influences how accurately the induced quantities are evaluated in various organs. Organs small in any dimension are poorly represented by large voxels. The maximum induced quantities are consistently higher as the voxel dimension decreases. The differences are typically of the order of 30–50% for voxels of 3.6 compared with 7.2 mm (Dawson, Caputa & Stuchly, 1998).

The main features of dosimetry for exposures to the ELF electric field can be summarized as follows.

- Magnitudes of the induced electric fields are typically 10^{-4} to 10^{-7} of the magnitude of external unperturbed field.

- Since the exposure is mostly to the vertical field, the predominant direction of the induced fields is also vertical.

- In the same exposure field, the strongest induced fields are for the human body in contact through the feet with a perfectly conducting ground plane, and the weakest induced fields are for the body in free space, i.e. infinitely far from the ground plane.

- The global dosimetric measure of short-circuit current for a body in contact with perfect ground is determined by the body size and shape (including posture) rather than tissue conductivity.

- The induced electric field values are to a lesser degree influenced by the conductivity of various organs and tissues than are the values of the induced current density.

Figure 4 shows vertical current computed in models of an adult and a child exposed to the vertical electric field in free space and in contact with perfect ground.

Table 23 gives various dosimetric measures for the human body model in a vertical field of 1 kV/m at 60 Hz (Dawson, Caputa & Stuchly, 1998; Kavet et al., 2001). Equivalent data for 50 Hz is shown in Table 24 (Dimbylow, 2005). In these calculations the body is in contact with perfectly conducting ground through both feet, the body height is 1.76 m for NORMAN and 1.63 m for NAOMI and weight is 73 kg for NORMAN and 60 kg for NAOMI. Table 25 gives dosimetric measures for a simplified model of a 5-year old child of 1.10 m and 18.7 kg (Hirata et al., 2001). The voxel maximum values in these models are significantly overestimated, thus 99th percentiles are more representative (Dawson, Potter & Stuchly, 2001).
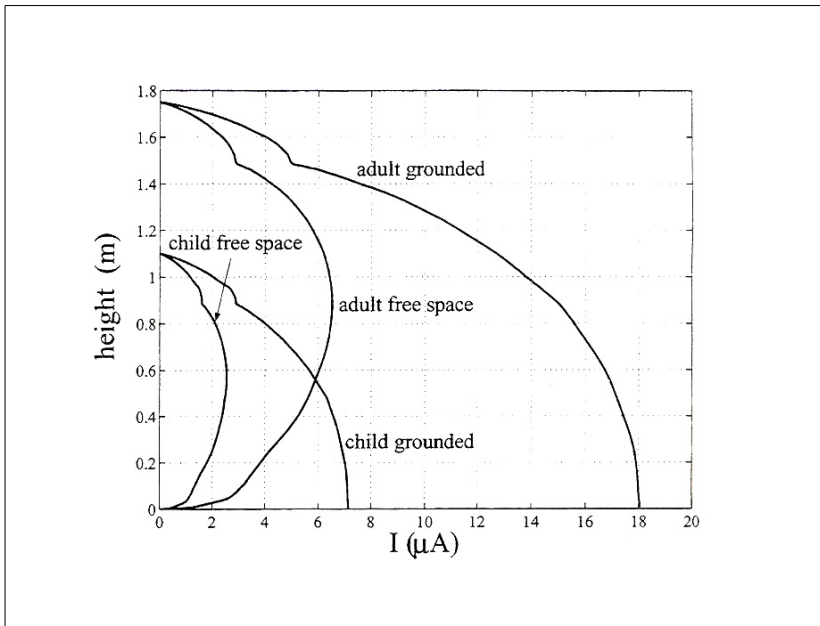
Figure 4. Current in body cross-sections for a human body model in contact with perfect ground at 1 kV m^{-1} and 60 Hz (Hirata et al., 2001).

Table 23. Induced electric fields (mV m^{-1}) of a grounded human body model in a vertical uniform electric field of 1 kV m^{-1} and 60 Hz[a] or 50 Hz[b]

Tissue/Organ	Mean		99th percentile		Maximum	
	50 Hz	60 Hz	50 Hz	60 Hz	50 Hz	60 Hz
Bone	5.72	3.55	49.4	34.4	88.8	40.8
Tendon	9.03		37.9		55.1	
Skin	2.74		33.1		67.3	
Fat	2.31		25.2		84.4	
Trabecular bone	2.80	3.55	15.1	34.4	56.5	40.8
Muscle	1.65	1.57	8.14	10.1	24.1	32.1
Bladder	1.86		6.49		8.58	
Prostate		1.68		2.81		3.05
Heart muscle	1.29	1.42	3.98	2.83	5.83	3.63
Spinal cord	1.16		2.92		4.88	
Liver	1.63		2.88		5.05	
Pancreas	1.09		2.76		6.03	
Lung	1.09	1.38	2.54	2.42	5.69	3.57

Table 23. Continued.

Spleen	1.33	1.79	2.49	2.61	5.07	3.22
Vagina	1.46		2.34		3.23	
Uterus	1.14		2.13		3.01	
Thyroid	1.16		2.03		3.29	
White matter	0.781	0.86	2.02	1.95	6.13	3.70
Kidney	1.29	1.44	1.86	3.12	4.10	4.47
Stomach	0.739		1.86		3.29	
Adrenals	1.35		1.83		2.32	
Ovaries	0.802		1.69		2.03	
Blood	0.690	1.43	1.66	8.91	3.06	23.8
Grey matter	0.474	0.86	1.62	1.95	4.85	3.70
Oesophagus	0.995		1.61		4.16	
Duodenum	0.765		1.60		2.92	
Lower LI	0.897		1.53		3.79	
Breast	0.705		1.46		2.68	
Gall bladder	0.439		1.36		2.03	
Small intestine	0.709		1.20		4.29	
CSF	0.271	0.35	1.15	1.02	2.38	1.58
Thymus	0.719		1.09		1.70	
Cartilage nose	0.598		1.03		1.40	
Upper LI	0.557		0.989		3.57	
Testes		0.48		1.19		1.63
Bile	0.352		0.805		1.26	
Urine	0.295		0.700		1.29	
Lunch	0.370		0.621		1.14	
Sclera	0.292		0.567		0.623	
Retina	0.314		0.552		0.582	
Humour	0.188		0.276		0.321	
Lens	0.211		0.268		0.268	

[a] Source: Dawson, Caputa & Stuchly, 1998; Kavet et al., 2001.

[b] Source: Dimbylow, 2005.

Table 24. Induced electric field for 99th percentile voxel value at 50 Hz for an applied electric field in a female phantom (NAOMI) and a male phantom (NOR-MAN). The external field is that required to produce a maximum induced electric field in the brain, spinal cord (sc) or retina of 100 mV m^1 [a]

Geometry	Electric field mV m^{-1} per kV m^{-1} for 99th percentile				External field (kV m^{-1})
	Brain	Spinal cord	Retina	Largest	
NAOMI, GRO [b]	2.02	2.92	0.552	2.92 sc	34.2
NORMAN, GRO	1.62	3.42	0.514	3.42 sc	29.2
NAOMI, ISO	1.22	1.40	0.336	1.40 sc	71.4
NORMAN, ISO	0.811	1.63	0.262	1.63 sc	61.3

[a] Source: Dimbylow, 2005.

[b] GRO: grounded; ISO: isolated.

Table 25. Induced electric fields (mV m^{-1}) of a grounded child body model in a vertical uniform electric field of 60 Hz, 1 kV m^{-1} [a]

Tissue/Organ	Mean	99th percentile	Maximum
Blood	1.52	9.18	18.06
Bone marrow	3.70	32.85	41.87
Brain	0.70	1.58	3.07
CSF	0.28	0.87	1.37
Heart	1.60	3.07	3.69
Lungs	1.55	2.63	3.69
Muscle	1.65	9.97	30.56

[a] Source: Hirata et al., 2001.

The current density averaged over 1 cm^2, which is the basic exposure unit in the ICNIRP guidelines (ICNIRP, 1998a), is illustrated in Figure 5.
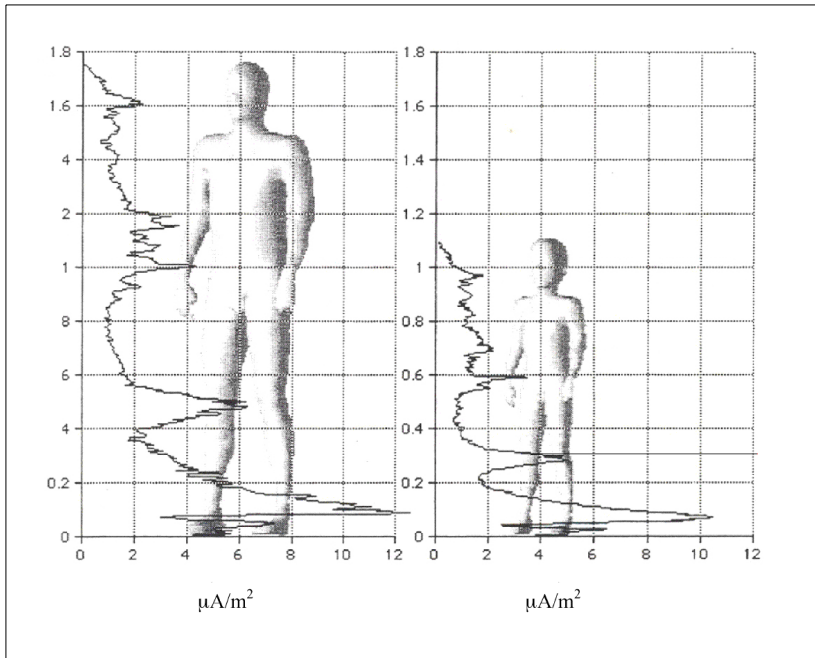
Figure 5. Maximum current density in μA m^{-2} averaged over 1 cm^2 in vertical body layers for grounded models exposed to a vertical electric field of 1 kV m^{-1} and 60 Hz (Hirata et al., 2001).

With certain exposures in occupational situations, e.g. in a substation, when the human body is close to a conductor at high potential, higher electric fields are induced in some organs (e.g. the brain) than calculated using the measured field 1.5 m above ground (Potter, Okoniewski & Stuchly, 2000). This is to be expected, as the external field increases above the ground.

3.3.4 Comparison of computations with measurements

Computed (Gandhi & Chen, 1992) and measured (Deno, 1977) current distributions for ungrounded and grounded human of 1.77 m height standing in a vertical homogeneous electric field are illustrated in Figure 6.
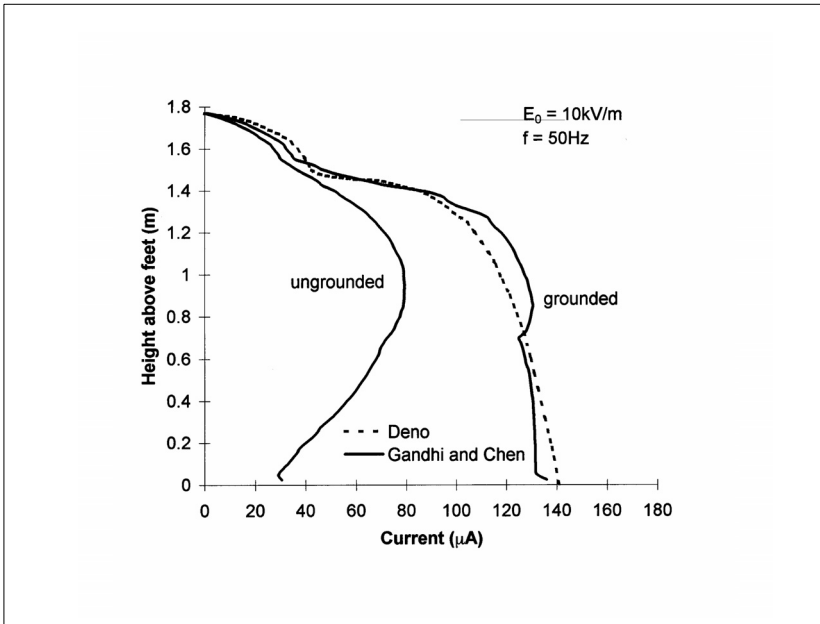
Figure 6. Computed (Gandhi & Chen, 1992) and measured (Deno, 1977) current distribution for an ungrounded and grounded human of 1.77 m in height standing in a vertical homogeneous electric field of 10 kV m^{-1} at 50 Hz.

Table 26 shows a comparison of the computed (Dawson, Caputa & Stuchly, 1998) vertical current across a few cross-sections of the human body with the measurements (Tenforde & Kaune, 1987). Given the modelling differences among the laboratories, the agreement can be considered very acceptable.

Table 26. Induced vertical current (µA) in a human body model in a vertical uniform electric field of 60 Hz and 1 kV m^{-1}

Body position	Grounded		Elevated above ground		Free space	
	Computed[a]	Measured[b]	Computed[a]	Measured[b]	Computed[a]	Measured[b]
Neck	4.9	5.4	3.7	4.0	2.9	3.1
Chest	9.8	13.5	7.0	8.7	5.3	5.4
Abdomen	13.8	14.6	9.1	9.3	6.6	5.7
Thigh	16.6	15.6	9.7	9.4	6.1	5.6
Ankle	17.6	17.0	7.3	8.0	3.0	3.0

[a] Source: Dawson, Caputa & Stuchly, 1998.

[b] Source: Tenforde & Kaune, 1987.

3.4 Magnetic field dosimetry

3.4.1 Basic interaction mechanisms

Human and animal bodies do not perturb the magnetic field, and the field in tissue is the same as the external field, since the magnetic permeability of tissues is the same as that of air. The quantities of magnetic material that are present in some tissues are so minute that they can be neglected in macroscopic dosimetry. The main interaction of a magnetic field with the body is the Faraday induction of an electric field and associated current in conductive tissue. In a homogeneous tissue the lines of electric flux (and current density) are solenoidal. In the case of heterogeneous tissues, consisting of regions of different conductivities, currents are flowing also at the interfaces between the regions. In the simplest model of an equivalent circular loop corresponding to a given body contour the induced electric field is

$$E = \pi \, f \, r \, B$$

and the current density is

$$J = \pi f \sigma r B$$

where f is the frequency, r is the loop radius and B is the magnetic flux density vector normal to the current loop. Similarly, ellipsoidal loops can be considered to better fit into the body shape.

Electric fields and currents induced in the human body cannot be measured easily. Measurements in animals have been performed, but data are limited, and the accuracy of measurements is relatively poor.

3.4.2 Computations – uniform field

Heterogeneous models of the human body similar to those used for electric field exposures have been numerically analyzed using the impedance method (IM) (Gandhi et al., 2001; Gandhi & Chen, 1992; Gandhi & DeFord, 1988), and the scalar potential finite difference (SPFD) technique (Dawson & Stuchly, 1996; Dimbylow, 1998). Even more extensive data than for the electric field are available for the magnetic field. The influence on the induced quantities of the model resolution, tissue properties in general and muscle anisotropy specifically, field orientation with respect to the body, and to a certain extent body anatomy have been investigated (Dawson, Caputa & Stuchly, 1997b; Dawson & Stuchly, 1998; Dimbylow, 1998; Stuchly & Dawson, 2000). In the past, the maximum current density in a body part has often been calculated using the largest loop of current that can be incorporated in it. Dawson, Caputa & Stuchly (1999b) have shown that induced parameters should be calculated for organs in situ instead of for isolated ones, since there is a significant influence of surrounding structures.

The main features of dosimetry for exposures to the uniform ELF magnetic field can be summarized as follows.

- The electric fields induced in the body depend on the orientation of the magnetic field with respect to the body.

- For most organs and tissues, as expected, the magnetic field orientation normal to the torso (front-to-back) gives maximum induced quantities.

- In the brain, cerebrospinal fluid, blood, heart, bladder, eyes and spinal cord, the highest quantities are induced by the magnetic field oriented side-to-side.

- Consistently lowest induced fields are for the magnetic field oriented along the vertical body axis.

- For a given field strength and orientation, greater electric fields are induced in a body of a larger size.

- The induced electric field values are to the lesser degree influenced by the conductivity of various organs and tissues than the values of the induced current density.

Table 27 presents electric field induced in several organs and tissues at 60 Hz, 1 µT magnetic field oriented front-to-back (Dawson, Caputa & Stuchly, 1997b; Dawson & Stuchly, 1998; Kavet et al., 2001). Comparable data at 50 Hz and normalized to 1 mT are shown in Table 28 (Dimbylow, 2005). An example of the current distribution in the body compared to the body anatomy is illustrated in Figure 7. The layer averaged electric field and current density for two sets of tissue conductivity are shown in Figure 8.

Table 27. Induced electric fields (mV m^{-1}) in the human body model in a uniform magnetic field of 1 mT and 60 Hz or 50 Hz oriented front-to-back [a]

Tissue/organ	Mean		99th percentile		Maximum	
	50 Hz	60 Hz	50 Hz	60 Hz	50 Hz	60 Hz
Bone	11.6	16	50.9	23	166	83
Tendon	2.81		9.35		14.9	
Skin	13.5		36.0		65.6	
Fat	13.7		33.5		129	
Trabecular bone	6.40	16	24.3	23	48.5	83
Muscle	8.44	15	23.0	51	67.6	147
Bladder	11.8		45.8		64.7	
Heart muscle	9.62	14	28.0	38	42.0	49
Spinal	8.90		27.0		53.0	
Liver	13.2		38.2		73.1	
Pancreas	3.52		13.6		24.9	
Lung	8.22	21	24.4	49	93.3	86
Spleen	8.16	41	18.4	72	27.2	92
Vagina	3.76		12.0		19.4	

Table 27. Continued.

Uterus	3.81		9.44		17.0	
Prostate		17		36		52
Thyroid	12.6		21.8		37.9	
White matter	10.1	11	31.4	31	82.5	74
Kidney	10.8	25	22.5	53	39.2	71
Stomach	4.52		15.0		26.8	
Adrenals	9.91		19.2		24.5	
Ovaries	2.40		5.30		7.87	
Blood	5.99	6.9	17.5	23	30.9	83
Grey matter	8.04	11	30.2	31	74.8	74
Oesophagus	4.86		10.0		14.1	
Duodenum	5.22		14.1		22.1	
Lower LI	4.30		12.2		27.4	
Testes		15		41		73
Breast	18.1		31.0		51.6	
Gall bladder	3.41		9.64		14.8	
Small intestine	3.98		10.4		24.8	
CSF	5.25	5.2	14.8	17	33.3	25
Thymus	12.2		19.6		30.7	
Cartilage nose	13.4		31.5		38.3	
Upper LI	5.85		12.7		21.1	
Bile	2.56		6.63		9.56	
Urine	2.16		4.71		7.55	
Lunch	2.31		6.47		7.58	
Sclera	7.78		16.3		18.2	
Retina	6.69		13.5		15.1	
Humour	4.51		7.41		9.20	
Lens	5.22		6.70		6.70	

[a] Sources: Dawson & Stuchly, 1998 (60 Hz), Dimbylow, 2005 (50 Hz).

Table 28. Induced electric field for 99th percentile voxel value at 50 Hz for an applied magnetic field in a female phantom (NAOMI) and a male phantom (NOR-MAN). The external field (in terms of magnetic flux density) is that required to produce a maximum induced electric field in the brain (br), spinal cord (sc) or retina of 100 mV m^{-1} [a]

Geometry	Induced electric field mV m^{-1} per mT for 99th percentile				External field (mT)
	Brain	Spinal cord	Retina	Largest	
NAOMI, AP [b]	25.7	17.7	6.98	25.7 br	3.89
NORMAN, AP	30.7	29.7	7.05	30.7 br	3.26
NAOMI, LAT	31.4	27.0	13.5	31.4 br	3.18
NORMAN, LAT	33.0	48.6	14.6	48.6 sc	2.06
NAOMI, TOP	25.1	8.60	6.90	25.1 br	3.98
NORMAN, TOP	22.1	23.0	10.2	23.0 sc	4.35

[a] Source: Dimbylow, 2005.

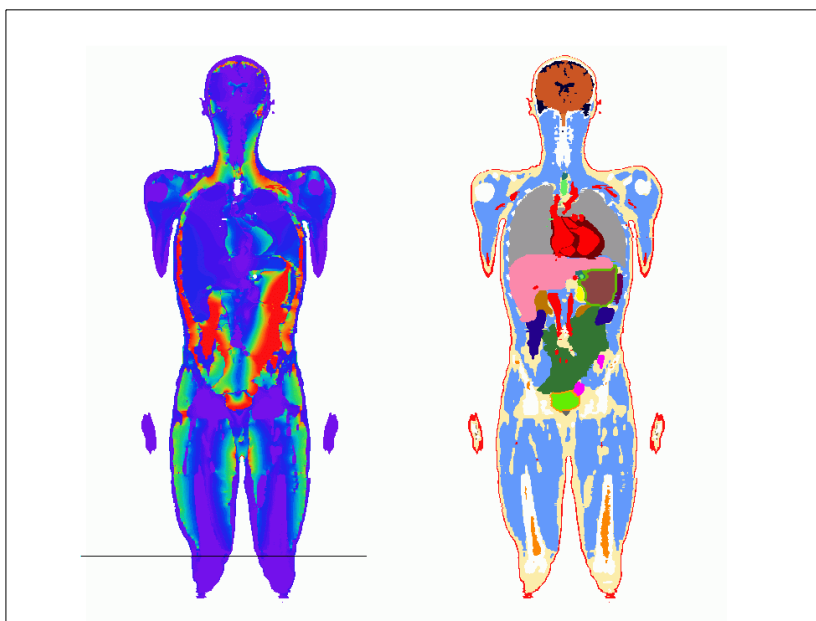[b] AP: front-to-back; LAT: side-to-side; TOP: head-to-feet.

Figure 7. Distribution of the current density (left) induced by a uniform magnetic field of 50 Hz perpendicular to the frontal plane, calculated for an anatomically shaped heterogeneous model of the human body (right) (Dimbylow, 1998). The colour map of the current density (left) is a spectrum, the highest values in red and the lowest values in violet, and is only intended to give a general view of current density patterns.
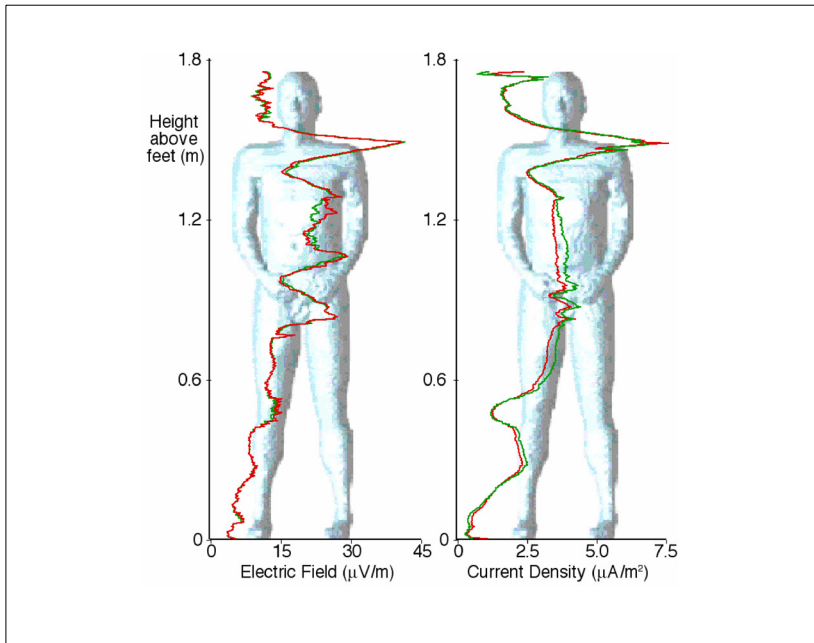
Figure 8. Layer-averaged magnitude of the electric field in V m^{-1} and current density in A m^{-2} for exposure to a uniform magnetic flux density of 1 µT and 60 Hz oriented front-to-back. The two curves on each graph correspond to two sets of conductivity (Dawson & Stuchly, 1998).

3.4.3   *Computations – non-uniform fields*

Human exposure to relatively high magnetic flux density values most often occurs in occupational settings. Numerical modeling has been considered mostly for workers exposed to high-voltage transmission lines (Baraton & Hutzler, 1995; Dawson, Caputa & Stuchly, 1999a; Dawson, Caputa & Stuchly, 1999c; Stuchly & Zhao, 1996). In those cases, current-carrying conductors can be represented as infinite straight-line sources. However, some of the exposures occur in more complex scenarios, two of which have been analyzed, a more-realistic representation of the source conductors based on finite line segments has been used (Dawson, Caputa & Stuchly, 1999d). Table 29 gives dosimetry for two representative exposure scenarios illustrated in Figure 9 (Dawson, Caputa & Stuchly, 1999c). Current in each conductor is 250 A for a total of 1000 A in a four-conductor bundle.
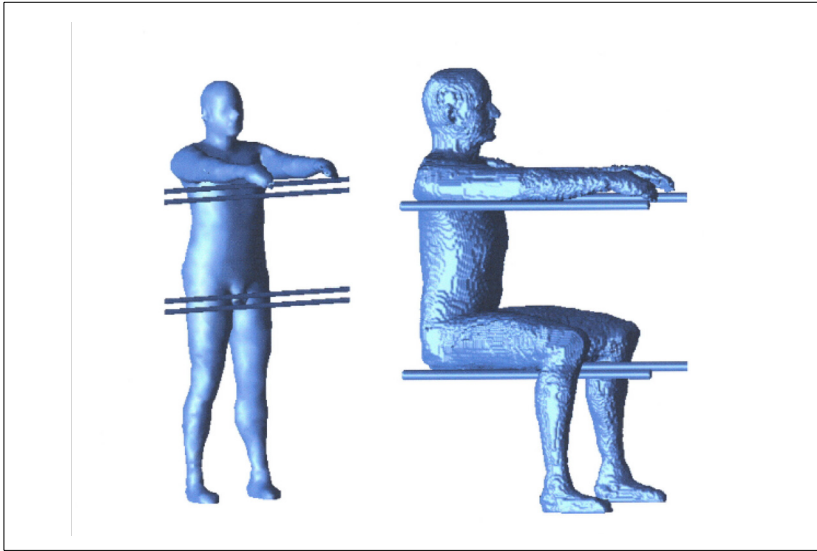
Figure 9. Two exposure scenarios used in calculations for workers exposed to high-voltage transmission lines (Dawson, Caputa & Stuchly, 1999c).

Table 29. Calculated electric fields (mV m^{-1}) induced in a model of an adult human for the occupational exposure scenarios shown in Figure 9 (total current in conductors: 1000 A; 60 Hz) [a]

Tissue/organ	Scenario A		Scenario B	
	E_{max}	E_{rms}	E_{max}	E_{rms}
Blood	20	3.7	15	2.4
Bone	90	11	58	7.2
Brain	22	4.6	28	5.9
Cerebrospinal fluid	9.2	2.3	14	3.7
Heart	27	11	9.0	3.2
Kidneys	22	7.9	2.8	0.9
Lungs	31	10	9.9	2.9
Muscle	59	6.9	33	5.5
Prostate	5.5	1.9	2.6	1.2
Testes	18	5.5	2.7	1.2

[a] Source: Stuchly & Dawson, 2000.

3.4.4   Computations – inter-laboratory comparison and model effects

To assess the reliability of data obtained by using anatomy based body models and numerical methods, an interlaboratory comparison was per-

formed (Caputa et al., 2002). Two groups in the UK and Canada used the 3.6 mm and 2 mm resolution models of average size. Each group applied its own, independently developed, field solver based on the Scalar Potential Finite Difference (SPFD) method. For a great majority of tissues, the difference in calculated parameters between the two groups was 1% or less. Only in a few cases it reaches 2–3 %. Differences of the order of 1–2 % are typically expected on the basis of the accuracy analysis (Dawson, Potter & Stuchly, 2001).

In addition, a larger size model was used to investigate effects of body size and anatomy (Caputa et al., 2002). The size of the body model and its shape (including anatomy and resolution) influenced the average (E_{avg}), voxel maximum and 99 percentile values of the induced electric field (E_{99}). The large size model mass was about 40% greater than that of the two average size models. Correspondingly, the whole-body-average electric fields were also about 40% greater, while 99 percentile electric fields were 41% and 34% greater. Such simple mass-based scaling did not apply even approximately to specific organs and tissues. The actual anatomy of persons represented by the models, as well as the accuracy of the models, both influenced differences in the two dosimetric measures for organs that are computed accurately, namely E_{avg} and E_{99}. The two models of similar size showed typically differences by about 10% or less in the average and 99 percentile values, e.g. E_{avg} in blood, brain, heart, kidney, muscle, and E_{99} in blood, brain, muscle, for the same model resolution. Relatively small organs, such as the testes, or thin organs, such as the spinal cord, indicated larger differences in induced electric field strengths that could be directly ascribed to the differences in the shape and size of these organs in the models.

3.5   Contact current

Contact currents produce electric fields in tissue that are similar to and often much greater than those induced by external electric and magnetic fields. Contact currents occur when a person touches conductive surfaces at different potentials and completes a path for current flow through the body. Typically, the current pathway is hand-to-hand and/or from a hand to one or both feet. Contact current sources may include the appliance chassis that, because of typical residential wiring practices (in North America), carry a small potential above a home ground. Also, large conductive objects situated in an electric field, such as a vehicle parked under a transmission line, serve as a source of contact current. The possible role of contact currents as a factor responsible for the reported association of magnetic fields with childhood leukaemia was first introduced by Kavet et al. (2000) in a scenario that involved contact with appliances. In subsequent papers, a more plausible exposure scenario has been developed that entails contact currents to children with low contact resistance while bathing and touching the water fixtures (Kavet et al., 2004; Kavet, 2005; Kavet & Zaffanella, 2002).

Recently, electric fields have been computed in an adult and a child model with electrodes on hands and feet simulating contact current (Dawson et al., 2001). Three scenarios are considered based on the combinations of

electrodes. In all scenarios contact is through one hand. In scenario A the opposite hand and both feet are grounded. In scenario B only the opposite hand is grounded. This scenario represents touching a charged object with one hand and grounded object with another hand. Scenario C has both feet grounded. This is perhaps the most common and represents touching an ungrounded object while both feet are grounded. Dosimetric measures can be scaled linearly for other contact current values. These in turn can be obtained for a given contact resistance (or impedance) for a known open-circuit voltage. Table 30 gives representative measures for the electric field in bone marrow, which do not vary significantly, for the three scenarios. The measures in the bone marrow are of interest in view of the reports by Kavet and colleagues cited above. It should be noted that the electric fields in the brain are negligibly small in the case of contact currents.

Table 30. Calculated electric field (mV m^{-1}) induced by a contact current of 60 Hz, 1 μA in voxels of bone marrow of a child [a]

Body part	E_{avg}	E_{99}
Lower arm	5.1	14.9
Upper arm	0.9	1.4
Whole body	0.4	3.3

[a] Source: Dawson et al., 2001.

Examination of data in Table 30 indicates that, averaged across the body, electric fields of the order of 1 mV m^{-1} are produced in bone marrow of children from a contact current of 1 μA. However, much higher values occur in the marrow of the lower contacting arm: 5 mV m^{-1} per μA averaged across this anatomical site and an upper 5th percentile of 13 mV m^{-1} per μA in this tissue. As discussed in section 4.6.2, 50 μA may result from the upper 4% of contact voltages measured between the water fixture and the drain (the site of exposure) in one US measurement study (Kavet et al., 2004); such a voltage would produce bone marrow doses of about 650 mV m^{-1} (see section 4.6.2). In contrast, current resulting from contact with an appliance would be very limited owing to the resistance of structural materials, shoes, and dry skin (Kavet et al., 2000). Contact with vehicle-sized objects in an electric field would produce currents in excess of roughly 5 μA per kV m^{-1} (Dawson et al., 2001), and would depend on the grounding of the vehicle relative to the contacting person's grounding.

3.6   Comparison of various exposures

It is interesting to compare different electric and magnetic field exposures that produce equivalent internal electric fields in different organs. Such comparisons are given in Table 31 based on published data (Dawson, Caputa & Stuchly, 1997a; Dimbylow, 2005; Stuchly & Dawson, 2002).

Table 31. Electric (grounded model) or magnetic field (front-to-back) source levels at 50 or 60 Hz needed to induce mean and maximum electric field of 1 mV m^{-1}, calculated from data of tables 23 and 27

Organ	Electric field (kV m^{-1})			
	Mean		99th percentile	
	50 Hz	60 Hz	50 Hz	60 Hz
Blood	1.45	0.70	0.60	0.11
Bone	0.17	0.28	0.020	0.029
Brain	1.28	1.16	0.50	0.51
CSF	3.69	2.86	0.87	0.98
Heart	0.78	0.70	0.25	0.35
Kidneys	0.78	0.69	0.54	0.32
Liver	0.61		0.35	
Lungs	0.92	0.72	0.39	0.41
Muscle	0.61	0.64	0.12	0.099
Prostate		0.60		0.36
Testes		2.08		0.84

Organ	Magnetic field (µT)			
	Mean		99th percentile	
	50 Hz	60 Hz	50 Hz	60 Hz
Blood	166.9	144.9	57.1	43.5
Bone	86.2	62.5	19.6	43.5
Brain	99.0	90.9	31.8	32.3
CSF	190.5	192.3	67.6	58.8
Heart	104.0	71.5	35.7	26.3
Kidneys	92.6	40.0	44.4	18.9
Liver	75.8		26.2	
Lungs	121.7	47.6	41.0	20.4
Muscle	118.5	66.7	43.5	19.6
Prostate		58.8		27.8
Testes		66.7		24.4

3.7 Microscopic dosimetry

Macroscopic dosimetry that gives induced electric fields in various organs and tissues can be extended to more spatially refined models of subcellular structures to quantitatively predict and understand biophysical interactions. The simplest subcellular modeling that considers linear systems requires evaluation of induced fields in various parts of a cell. Such models, for instance, have been developed to understand neural stimulation (Abdeen & Stuchly, 1994; Basser & Roth, 1991; Malmivuo & Plonsey, 1995; Plonsey

& Barr, 1988; Reilly, 1992). Also, in the past, simplified models of cells consisting of a membrane, cytoplasm and nucleus, and suspended in conductive medium have been considered (Foster & Schwan, 1989). The membrane potential has been computed for spherical (Foster & Schwan, 1996), ellipsoidal (Bernhardt & Pauly, 1973) and spheroidal cells (Jerry, Popel & Brownell, 1996) suspended in a lossy medium. Computations are available as a function of the applied electric field and its frequency. Because cell membranes have high resistivity and capacitance (nearly constant for all mammalian cells and equal to 1 F cm^{-2}), at sufficiently low frequencies high fields are produced at the two faces of the membrane. The field is nearly zero inside the cell, as long as the frequency of the applied field is below the membrane relaxation frequency. This specific relaxation frequency depends on the total membrane resistance and capacitance. The larger the cell, the higher the induced membrane potential for the same applied field. However, the larger the cell, the lower the membrane relaxation frequency.

Gap junctions connect most cells. A gap junction is an aqueous pore or channel through which neighboring cell membranes are connected. Thus, cells can exchange ions, for example, providing local intercellular communication (Holder, Elmore & Barrett, 1993). Certain cancer promoters inhibit gap communication and allow the cells to multiply uncontrollably. It has been hypothesized with support from some suggestive experimental results, that low-frequency electric and magnetic fields may affect intercellular communication. Gap-connected cells have previously been modeled as long cables (Cooper, 1984). Also, very simplified models have been used, in which gap-connected cells are represented by large cells of the size of the gap-connected cell-assemblies (Polk, 1992). With such models relatively large induced membrane potentials have been estimated, even for moderate applied fields.

A numerical analysis has been performed to compute membrane potentials in more realistic models (Fear & Stuchly, 1998a; 1998b; 1998c). Various assemblies of cells connected by gap-junctions have been modeled with cell and gap-junction dimensions and conductivity values representative of mammalian cells. These simulations have indicated that simplified models can only be used for some specific situations. However, even in those cases, equivalent cells have to be constructed in which cytoplasm properties are modified to account for the properties of gap-junctions. These models predict reasonably well the results for very small assemblies of cells of certain shapes and at very low frequencies (Fear & Stuchly, 1998b). On the other hand, numerical analysis can predict correctly the induced membrane potential as well as the relaxation frequency (Fear & Stuchly, 1998a; 1998c). It has been shown that, as the size of the cell-assembly increases, the membrane potential even at DC does not increase linearly with dimensions, as it does for very short elongated assemblies. There is a characteristic length for elongated assemblies beyond which the membrane potential does not increase significantly. There is also a limit of increase for the membrane potential for assemblies of other shapes. Even more importantly, as the assembly size

(volume) increases, the relaxation frequency decreases (at the relaxation frequency the induced membrane potential is half of that at DC).

From this linear model of gap-connected cells, it is concluded that at 50 or 60 Hz the induced membrane potential in any organ of the human body exposed to a uniform magnetic flux density of up to 1 mT or to an electric field of approximately 10 kV m^{-1} or less, does not exceed 0.1 mV. This is small in comparison to the endogenous resting membrane potential in the range 20-100 mV.

3.8   Conclusions

Exposure to external electric and magnetic fields at extremely low frequencies induces electric fields and currents inside the body. Dosimetry describes the relationship between the external fields and the induced electric field and current density in the body, or other parameters associated with exposure to these fields. The local induced electric field and current density are of particular interest because they relate to the stimulation of excitable tissue such as nerve and muscle.

The bodies of humans and animals significantly perturb the spatial distribution of an ELF electric field. At low frequencies the body is a good conductor and the perturbed field lines outside the the body are nearly normal to the body surface. Oscillating charges are induced on the surface of the exposed body and these induce currents inside the body. The key features of dosimetry for the exposure of humans to ELF electric fields are as follows:

- The electric field inside the body is normally five to six orders of magnitude smaller than the external electric field.

- When exposure is mostly to the vertical field, the predominant direction of the induced fields is also vertical.

- For a given external electric field, the strongest induced fields are for the human body in perfect contact through the feet with the ground (electrically grounded) and the weakest induced fields are for the body insulated from the ground (in "free space").

- The total current flowing in a body in perfect contact with ground is determined by the body size and shape (including posture) rather than tissue conductivity.

- The distribution of induced currents across the various organs and tissues is determined by the conductivity of those tissues.

- The distribution of an induced electric field is also influenced by the conductivities, but less so than the induced current.

- There is also a separate phenomenon in which the current in the body is produced by means of contact with a conductive object located in an electric field.

For magnetic fields, the permeability of tissues is the same as that of air, so the field in tissue is the same as the external field. The bodies of

humans and animals do not significantly perturb the field. The main interaction of magnetic fields with the body is the Faraday induction of electric fields and associated current densities in the conductive tissues. The key features of dosimetry for the exposure to ELF magnetic fields are as follows:

- The induced electric field and current depend on the orientation of the external field. Induced fields in the body as a whole are greatest when the fields are aligned from the front or back of the body, but for some individual organs the highest values are induced for the field aligned from side-to-side.

- The consistently lowest induced electric fields are found when the external magnetic field is oriented along the vertical body axis.

- For a given magnetic field strength and orientation, higher electric fields are induced in a body of a larger size.

- The distribution of the induced electric field values is affected by the conductivity of various organs and tissues. These have a limited effect on the distribution of the induced current density.